

Current-voltage characteristics of seven-helix proteins from a cubic array of amino acids

Eleonora Alfinito*

Dipartimento di Ingegneria dell'Innovazione, Università del Salento, via Monteroni, I-73100 Lecce, Italy

Lino Reggiani†

*Dipartimento di Matematica e Fisica, "Ennio de Giorgi",
Università del Salento, via Monteroni, I-73100 Lecce, Italy*

(Dated: February 11, 2020)

The electrical properties of a set of seven-helix transmembrane proteins, whose space arrangement (3d structure) is known, are investigated by using regular arrays of the amino acids. These structures, specifically cubes, have topological features similar to those shown by the chosen proteins. The theoretical results show a good agreement between the predicted current-voltage characteristics obtained from a cubic array and those obtained from a detailed 3D structure. The agreement is confirmed by available experiments on bacteriorhodopsin. Furthermore, all the analyzed proteins are found to share the same critical behaviour of the voltage-dependent conductance and of its variance. In particular, the cubic arrangement evidences a short plateau of the excess conductance and its variance at high voltages. The results of the present investigation show the possibility to predict the I-V characteristics of multiple-protein sample even in the absence of a detailed knowledge of their 3D structure.

I. INTRODUCTION

The interest in the structure and function of a given protein is crossing the boundaries of biology, joining to electronics, applied physics and engineering. This relevant example of cross-fertilization is due to the quest of finding new and more efficient materials to produce green and renewable fuels [1, 2], to reduce wasting [3], to design highly specific prostheses for medicine [4, 5], to insure human and animal safety [6, 7]. Proteins perform *in vivo* activities that, when introduced in electronic devices, should allow astonishing performances [8, 9]. In particular, many transmembrane proteins act as highly specialized sensors, with levels of sensitivity and selectivity inconceivable for any artifact. The use of proteins in nano-bio-devices is, therefore, the topic of an emerging branch of electronics, recently introduced as proteotronics[10]. Proteotronics has the final objective of producing user-friendly, versatile devices for the daily life so as point-of-care testings and low invasive devices for medicine. As a matter of fact, the final device is conceived to be small and able to produce a clear response. This is allowed by the use of quite small active elements (protein samples), and an appropriate miniaturized electronic interface able to convert a biochemical response into an electrical signal. Recent experiments have shown how the capture mechanism of a ligand (small molecules, odours, photons, etc.) has a solid conjecture concerning the expected protein electrical responses [6, 11–14]. The microscopic interpretation is actually based on the knowledge of the detailed tertiary structure of the single

protein, i.e. of the space location of its amino acids. However, from one hand, such a knowledge is largely incomplete and even in the few favorable cases is still a matter of active research far from a general consensus in the scientific community [15]. From another hand, this knowledge is an essential input for modeling the charge transport of protein-based devices [11, 14, 16–19]. Indeed, the specific protein topology produces an electrical response very peculiar of the given protein [6, 11, 14, 16]. Thus, when this input is not known from a credited source, an approximate structure template able to reproduce the essential features of the electrical response, can be useful to model the protein electrical properties. In particular, we conjecture that for proteins with similar size and shape (globular, fibrous, transmembrane, etc.) the general trend of the electrical response or, at least, of the current-voltage (I-V) characteristic, can be modeled by using a single template.

The aim of this paper is to test the above conjecture. To this purpose, we have investigated three proteins belonging to the transmembrane family whose model of the tertiary structure (hereafter simply indicated as the 3D structure) is known [15, 20]. For one of them, the bacteriorhodopsin (bR), the I-V characteristic is also available from experiments[14, 21]. For these proteins the I-V characteristic has been calculated using an impedance network protein analogue (INPA) [10, 18]. The results obtained from the 3D structure have been compared with those obtained by using a regular structure, here taken as a cube, and proved to capture the main features of the protein electrical properties. The simple cube is built with a number of nodes as close as possible to the number of amino acids given by the public data bank (PDB) [15]. At present only the response corresponding to the protein native state will be analyzed. The presence of the ligand modifies the protein structure and also its free

* eleonora.alfinito@unisalento.it; <http://cmtg1.unile.it/eleonora1.html>

† lino.reggiani@unisalento.it

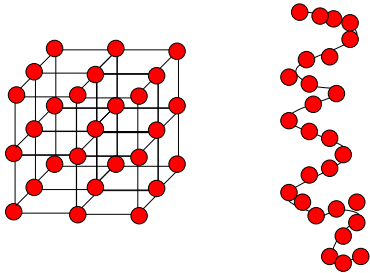


FIG. 1. Cartoon (not to scale) of the *cube3* and of an amino acid helix. Both structures have the same number of nodes.

energy [19] and this is beyond the aims of this paper.

The paper is organized as follows. In section II the theoretical model is briefly recalled. In section III the given proteins and the analogue cubic structures are introduced. Section IV reports the main results of this study and final conclusions are summarized in Sec. V.

II. MODEL

The microscopic approach makes use of the INPA model that describes the single protein electrical properties starting from the protein topology. The model was already detailed in previous papers [19, 22, 23] In particular, the amino acid space position, as given by the 3D protein structure, is used to build up a graph, where each node corresponds to an amino acid. Two nodes are then linked if their distance is below a cut-off value, R_C . Finally, the links are converted into elemental impedances, with the ensemble of impedances leading to an impedance network specific to describe the electrical properties of the single proteins. By appropriate scaling, the result of the single protein are compared with available experiments carried out on macroscopic samples.

In the present case, since the objective is the static I-V characteristic, the impedances reduce to resistances. The observed current response in monolayers of bR validates a tunneling-like mechanism of charge transport, which has been successfully simulated by using a Monte Carlo technique [18, 25, 26]. The model describes the observed transition between a quasi-linear (Ohmic) regime at low bias, ruled by the direct tunneling mechanism (DT), and a super-Ohmic regime at high bias, mostly due to the injection or Fowler-Nordheim (FN) tunneling mechanism. The critical value of the bias controlling the cross-over between the regimes, V_C , depends on the network structure and corresponds to a microscopic barrier height, Φ , taken to be independent from the specific structure. The

estimated value is $\Phi = 216meV$ [18].

The transition probability for tunneling assumes the standard form:

$$P_{i,j}^{\text{DT}} = \exp \left[-\alpha \sqrt{\left(\Phi - \frac{1}{2} eV_{i,j} \right)} \right] \quad (1)$$

if ($eV_{i,j} < \Phi$),

$$P_{i,j}^{\text{FN}} = \exp \left[-\alpha \frac{\Phi}{eV_{i,j}} \sqrt{\frac{\Phi}{2}} \right] \quad (2)$$

if ($eV_{i,j} \geq \Phi$)

where $V_{i,j}$ is the potential drop between the couple of i, j amino acids, $\alpha = \frac{2l_{i,j}\sqrt{2m}}{\hbar}$, and m is the electron effective mass, here taken the same of the bare value. When the FN tunneling is applicable ($eV_{i,j} \geq \Phi$), the maximal resistivity decreases, following the rule:

$$\rho(V) = \rho_{\text{MAX}} \left(\frac{\Phi}{eV_{i,j}} \right) + \rho_{\text{min}} \left(1 - \frac{\Phi}{eV_{i,j}} \right) \quad (3)$$

where $\rho_{\text{MAX}} = 4 \times 10^{13} \Omega \text{ \AA}$ is the maximum value of resistivity taken to fit the I-V characteristic at the lowest bias, and $\rho_{\text{min}} = 4 \times 10^5 \Omega \text{ \AA}$ the minimum resistivity value taken to fit the I-V characteristic at the highest voltages.

III. MATERIALS

We have analyzed three proteins, namely: bacteriorhodopsin (bR), rat olfactory receptor (OR) I7, and bovine rhodopsin (BR), all in their native state, i.e. the state pertaining to the protein in the absence of a specific external stimulus (ground state) [19]. As a consequence of an external stimulus, these proteins may change their native state into an active state. Bacteriorhodopsin is analyzed by using its 3D structure, as given by public PDB, in particular the 2NTU entry[15]. This structure consists of 222 amino acids, exhibits seven helices arranged to form a loop and has a size of about 5,5 nm. *Cube6*, the corresponding regular structure, consists of 6 nodes for edge, making a total of 216 nodes. The distance between contiguous nodes, the *gen*, is chosen of 5,5 Å which corresponds to a relative maximum of the bR amino acid distance distribution. With an analogous procedure the rat OR I7, whose 3D structure consists of 327 amino acids [20], is compared with the *cube7*, the corresponding regular structure that consists of 7 nodes for edge, making a total of 343 nodes with *gen*=5,5 Å. In both these cases, the value of the interaction radius, R_C , has been chosen of 6 Å as reported in previous papers [27, 28]. The same is done for BR, whose 3D structure consists of 348 amino acids, and the comparison is carried out with the *cube7*.

A cartoon of *cube3* with 3 nodes for edge, and an α -helix with the same number of amino acids (27) is shown in Fig. 1.

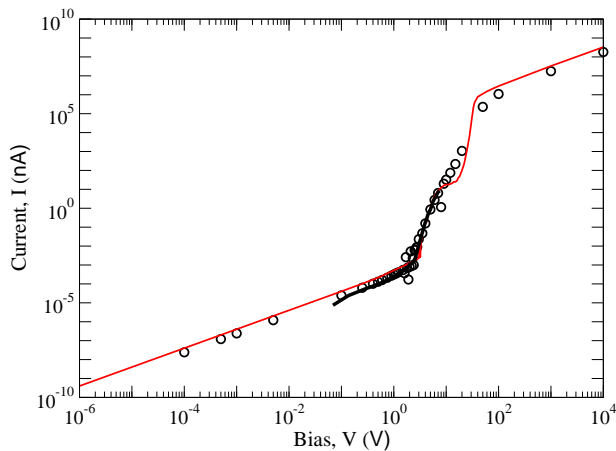


FIG. 2. I-V characteristics of bacteriorhodopsin (empty circles) and *cube6* (continuous red line), $R_C=6\text{\AA}$. The bold black line indicates the experimental data [21], color online.

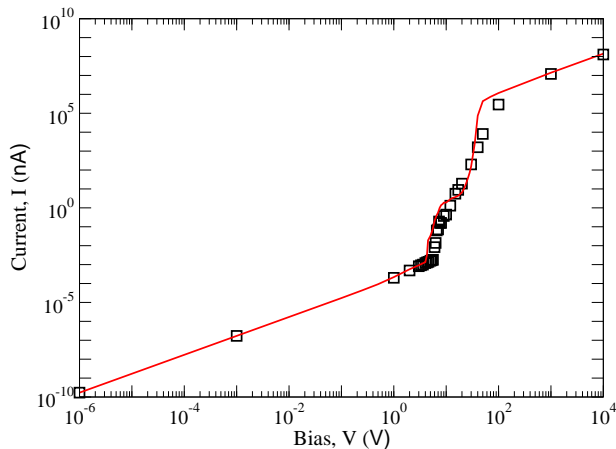


FIG. 3. I-V characteristics of rat OR I7 (empty squares) and *cube7* (continuous red line), $R_C = 6\text{\AA}$, color online.

IV. RESULTS

The calculated I-V characteristics of *cube6* and bR and of *cube7* and rat OR-I7 are reported in Fig. 2 and Fig. 3, respectively.

In Fig. 2 available experimental data [18, 21] are also shown. To our knowledge, the measurement of the I-V characteristics on rat OR-I7 samples do not have been performed, yet. In both cases calculations by using the 3D structure models for these proteins is well reproduced by the corresponding cubes, as well as the DT-FN transition. The specific critical bias values are summarized in Tab. I.

The normalized excess conductance, $\Gamma = (\langle g \rangle - g_0) / g_{max}$, is here taken as the order parameter that describes the associated phase transition between the DT and FN regimes. With this definition, Γ assumes a value in the interval $(0, 1)$. The normalization is performed by using g_0 , the lowest conductance value

(taken at the bias value of 10^{-6} V) and g_{max} , the highest conductance value (taken at the bias value of 10^4 V) which corresponds to the asymptotic Ohmic behaviour when all the resistivities of the network take the minimum value.

Close to the phase transition, the order parameter calculated for bR and rat OR I7 exhibits a power-law behaviour, when plotted as a function of the reduced bias, $\epsilon = (V - V_C) / V_C$. These results are reported in Fig. 4. As is usual in finite-size systems and due to the large fluctuations, rounding and shifting effects [29] do not allow to exactly pinpoint the phase transition. Furthermore, since the DT regime overlaps with the FN regime near the transition region, there can be identified two different "critical" bias values, V_C and V_G [26]. The critical bias V_C signals the beginning of the FN regime, where the system starts to deviate from the Ohmic behaviour [26], while V_G , the Ginzburg voltage [26, 30], indicates the consolidation of the FN regime.

A further signal of the existence of a universal behaviour is found by analyzing the scaled variance $(\langle g^2 \rangle - \langle g \rangle^2) / \langle g \rangle^2$. As just observed by analyzing different proteins [26], this quantity shows a power law with a critical exponent close to 3. Results are reported in Fig. 5. From the figures above it also emerges that, better than the current, Γ reveals the main differences between the 3D and the cube structure. Indeed, while the former shows a continuous increase after the DT-FN transition, the latter exhibits a plateau at intermediate bias. We suggest that this plateau is associated with the better regularity of the cube with respect to the 3D structure. As a matter of fact, by choosing $gen = 5, 5 \text{\AA}$, and $R_C = 6 \text{\AA}$, all the links have the same length and the pattern of potential barriers has itself a cubic shape. Conversely, in 3D structures the branches have a wide range of lengths and resistances. Therefore, as the bias increases (over the FN regime), at least one link able to get the lowest resistivity is available. Thus the transition toward the final Ohmic regime takes place continuously. Conversely, in the chosen cubic structures, the same bias increase produces a stalemate: all the branches have the same resistance value and none of them is able to prevail and gain the minimal resistivity. As a consequence, a kind of critical slowing down is observed at about $3V_C$. Finally, this condition is broken and all the branches achieve the minimal resistivity, and a percolation-like transition is observed. This analysis is represented in figure 6, where the scaled resistance, R/R_{MAX} , is reported both for *cube6* and *cube7*. A similar result was obtained by simulating colossal magnetoresistance in a regular 2D spin lattice, with electrons jumping potential barriers placed in all the sites [31]. Also in that case, the signature of a percolation transition was identified.

As a third case of interest, the bovine rhodopsin (BR) has been analyzed. This protein 3D structure, entry 1U19 of

| | Cube6 | bR | Cube7 | OR I7 | BR |
|--------------|-------|-----|-------|-------|------|
| V_C | 2,1 | 1,7 | 2,6 | 3,8 | 10 |
| <i>links</i> | 540 | 692 | 882 | 1005 | 1034 |
| <i>nodes</i> | 216 | 222 | 343 | 327 | 348 |

TABLE I. The critical bias V_C , links and nodes for the analyzed structures. Voltages are given in Volts, $R_C=6\text{\AA}$.

| | Cube7 | OR I7 | BR |
|--------------|-------|-------|------|
| V_C | 2,6 | 1,4 | 2,6 |
| <i>links</i> | 882 | 1339 | 1417 |
| <i>nodes</i> | 327 | 343 | 348 |

TABLE II. The critical bias V_C , links and nodes for the analyzed structures. Voltages are given in Volts, $R_C=7\text{\AA}$.

PDB, consists of 348 amino acids, similar to the rat OR I7. Therefore, its I-V characteristics should be also described by the *cube7*. This protein entry gives a structure a little bit more dilated than that of rat OR I7 and the I-V calculated by using $R_C = 6 \text{\AA}$ exhibits the value $V_C = 10 \text{ V}$, significantly larger when compared with the $V_C = 2,6 \text{ V}$ value obtained with *cube7*, $R_C = 6 \text{\AA}$ (see Tab. I). On the other hand, by increasing the value of R_C to 7\AA , both the 3D structure and the *cube7* give the same value for V_C , similar to that calculated for rat OR I7 by using $R_C = 7 \text{\AA}$. Notice that the results obtained with the cube structure are quite insensitive to the change of the R_C value inside the range ($gen, \sqrt{2}gen$). Results are reported in Fig. 7 and Table II.

In summary, we have found that proteins with a similar number of amino acids exhibit similar I-V characteristics, well reproduced by the cubic structure with $gen=5,5\text{\AA}$. The choice of a value of $R_C = 6$ or 7\AA , is irrelevant for

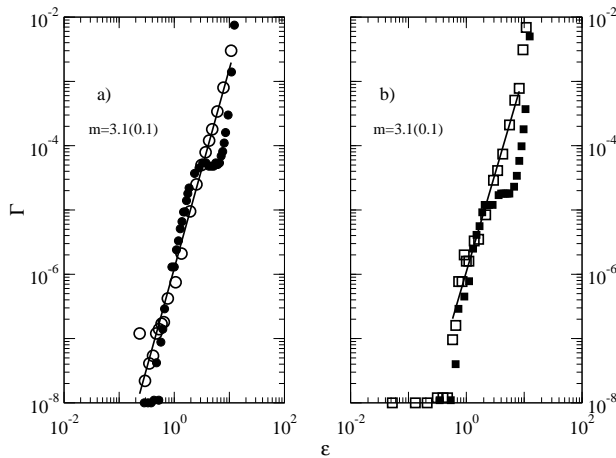
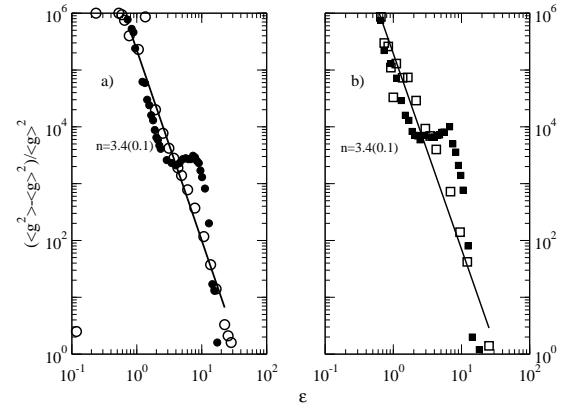


FIG. 4. a) Excess conductance for *cube6* (full circles) and bR (open circles), with $R_C=6 \text{\AA}$; b) Excess conductance for *cube7* (full squares) and OR-I7 (open squares), with $R_C=6 \text{\AA}$



$m=3.35(0.09)$

$m=3.37(0.04)$

FIG. 5. Scaled conductance variance. a) bR, empty circles, and *cube6*, full circles; b) rat OR I7, empty squares, and *cube7*, full squares.

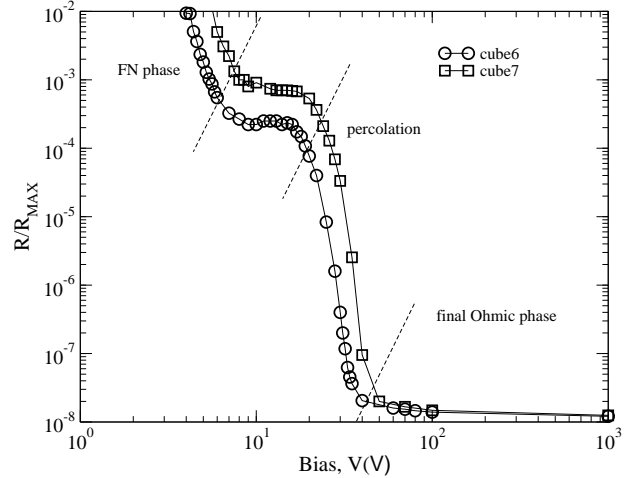


FIG. 6. Normalized resistances of *cube6* and *cube7*.

the cubic structure, which produces similar responses, but is noteworthy for the 3D structures.

V. CONCLUSIONS

The I-V characteristics of three seven-helix proteins, taken as a prototypes of this family, have been investigated within an INPA model. A comparative analysis between the 3D structure and a cubic arrangement of the amino acids is then carried out. The analysis shows a general agreement between the results of the 3D structures and those of the cubic arrays that contain a similar number of amino acids. In particular, the strong non-linearity of the I-V characteristic is well reproduced, to-

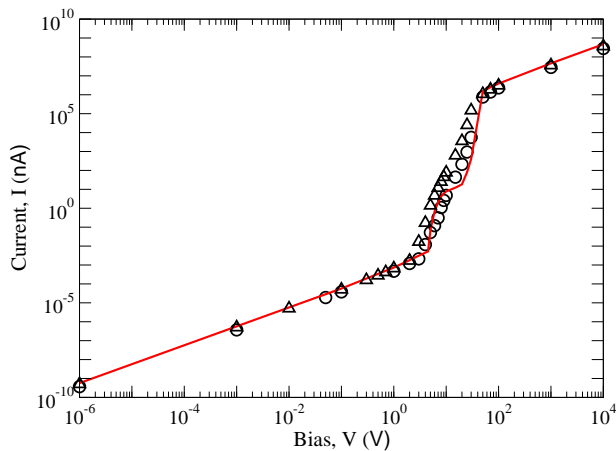


FIG. 7. I-V characteristics of BR (circles), rat OR I7 (triangles) and *cube7* (continuous red line), $R_C = 7\text{\AA}$, color online.

gether with some interesting peculiarities related to the phase transition between a direct and injection tunneling regime of charge transport. Accordingly, a cubic protein structure in the form presented here should provide realistic expectations of the I-V characteristics ascribed to a given protein even in the absence of a detailed knowledge of its 3D structure, thus being of valuable help to predict macroscopic electrical properties. A further step towards the advancing of proteotronics.

ACKNOWLEDGMENTS

This research is supported by the European Commission under the Bioelectronic Olfactory Neuron Device (BOND) project within the grant agreement number 228685-2.

-
- [1] C. King, B. Barbiellini, D. Moser and V. Renugopalakrishnan, *Phys. Rev. B* **85**, 125106 (2012)
- [2] V. Renugopalakrishnan, B. Barbiellini, C. King, M. Molinari, K. Mochalov, A. Sukhanova, ... and S. Ramakrishna, *J.Phys. Chem. C* **118**, 16710-16717 (2014).
- [3] G. Dai, L.M. Chao, and T. Iwasa, *Adv. Mat. Res.* **955**, 415 (2014).
- [4] P. Saaedi, J. M. Moosaabadi, M. Behmanesh, A. Eidi, and J. F. Mehrabadi, *J. Paramed Sci.* **2**, 2008 (2011).
- [5] D. Ghezzi, M. R. Antognazza, R. Maccarone, S. Bellani, E. Lanzarini, N. Martino, ... and F. Benfenati, *Nature Photonics* **7**, 400 (2013).
- [6] S. H. Lee, H. J. Jin, H. S. Song, S. Hong and T. H. Park, *J. Biotechnology* **157**, 467-472 (2012)
- [7] Z. Guo, N. Zine, F. Lagarde, J. Daligault, M.-A. Persuy, E. Pajot-Augy, A. Zhang, and N. Jaffrezic-Renault. *Food chemistry* **184**, 1 (2015).
- [8] U. Gether and B.K. Kobilka, *J. Bio. Chem.* **273**, 17979-17082 (1998)
- [9] S. L. Ritter, , and R. A. Hall. *Nature Rev. Mol. Cell Bio.* **10**, 819-830 (2009) .
- [10] E. Alfinito, L. Reggiani, and J. Pousset, "Proteotronics: Electronic Devices Based on Proteins." In *Sensors*, pp. 3-7. Springer International Publishing, 2015; E. Alfinito, J. Pousset, and L. Reggiani *Protein-Based Electronics: Transport Properties and Application. Towards the Development of a Proteotronics* (Pan Stanford Publishing Pte. Ltd. Penthouse Level, Suntec Tower 3 8 Temasek Boulevard Singapore 038988, in press) 9789814613637
- [11] Y. Hou, N. Jaffrezic-Renault, C. Martelet, A. Zhang, J. Minic-Vidic, T. Gorojankina, M.-A. Persuy, *et al*, *Bios. Bioelectr.* **22**, 1550-1555 (2007).
- [12] E. Alfinito and L. Reggiani, *J. Phys: Conf. Ser.* **193**(1), 012107 (2009).
- [13] I. Ron, L. Sepunaru, S. Itzhakov, T. Belenkova, N. Friedman, I. Pecht, *et al*, *J. Am. Chem. Soc.* **132**, 4131 (2010).
- [14] Y. Jin, N. Friedman, M. Sheves M, T. He, and D. Cahen, *Proc. Natl. Am. Soc.* **103**, 8601 (2006).
- [15] H. M. Berman, J. Westbrook, Z. Feng, G. Gilliland, T. N. Bhat, H. Weissig, I. N. Shindyalov, and P. E. Bourne, *Nucleic acids research* **28**, 235-242 (2000).
- [16] H. Melikyan, B.-E. Khishigbadrakh, A. Babajanyan, K. Lee, Ah-R. Choi, J.-Ha Lee, K.-H. Jung, and B. Friedman, *Thin Solid Films* **519**, 3425-3429 (2011).
- [17] E. Alfinito and L. Reggiani, *Europhys. Lett.* **85**, 68002 (2009).
- [18] E. Alfinito, J. -F. Millithaler, and L. Reggiani, *Phys. Rev. E* **83**, 042902 (2011).
- [19] E. Alfinito, and L. Reggiani, *Phys. Rev. E* **91**, 032702 (2015).
- [20] E. Alfinito, C. Pennetta, and L. Reggiani, *J. Appl. Phys.* **105**, 084703 (2009).
- [21] I. Casuso, L. Fumagalli, J. Samitier, E. Padròs, L. Reggiani L, V. Akimov, and G. Gomila, *Phys. Rev. E* **76**, 041919 (2007).
- [22] E. Alfinito, J. -F. Millithaler, and L. Reggiani, *Fluct. Noise Lett.* **11**, 1242005 (2012).
- [23] J.-F. Millithaler, E. Alfinito, and L. Reggiani, Charge transport and current fluctuations in bacteriorhodopsin based nanodevices. In: *Noise and Fluctuations (ICNF)*, 2011 21st International Conference on. IEEE, 2011. p. 417-420.
- [24] E. Alfinito, J. Pousset, and L. Reggiani, *J. Phys. Conf. Ser.* **490**, 012134 (2014).
- [25] E. Alfinito, and L. Reggiani *Phys. Rev. E* **81**, 032902 (2010).
- [26] E. Alfinito and L. Reggiani, *J. Phys: Condens. Matter* **25**, 375103 (2013); E. Alfinito, J. Pousset, and L. Reggiani, "Non-Gaussian fluctuations in opsins." In *Noise and Fluctuations (ICNF)*, 2013 22nd International Conference on, pp. 1-4. IEEE, 2013.
- [27] E. Alfinito, and L. Reggiani, *J. Appl. Phys.* **116**, 064901 (2014).
- [28] E. Alfinito, J. -F. Millithaler, and L. Reggiani, *Meas. Sci Technol.* **22**, 124004 (2011).
- [29] K. Binder, and D. P. Landau, *Phys. Rev. B* **13**, 1140 (1976).

- [30] E. Alfinito, and G. Vitiello, Phys. Rev. B **65**, 054105 (2002).
- [31] N.Vandewalle, M. Ausloos, and R. Cloots, Phys. Rev. B **59**, 11909 (1999)